DONG THAP UNIVERSITY JOURNAL OF SCIENCE
Tạp chí Khoa học Đại học Đồng Tháp
Natural Sciences Issue
ISSN 0866-7675 | e-ISSN 2815-567X

DOI: https://doi.org/10.52714/dthu.ns.2371.1829

ELECTRONIC STATES OF NODAL-LINE SEMIMETAL UNDER MAGNETIC FIELD

Bui Ngoc Thu[1] and Huynh Vinh Phuc[2]*

[1]Post-graduate student, Dong Thap University, Cao Lanh 870000, Vietnam

[2]Faculty of Natural Sciences Teacher Education, School of Education, Dong Thap University, Cao Lanh 870000, Vietnam

**Corresponding author, Email: hvphuc@dthu.edu.vn*

Article history

Received: 06/5/2025; Received in revised form: 26/6/2025; Accepted: 28/6/2025

Abstract

Nodal-line semimetals (NLSMs) have attracted significant attention due to their unique electronic properties arising from one-dimensional band degeneracies in momentum space. This study, we investigate the electronic states of NLSMs under the influence of a uniform external magnetic field. By formulating and solving the Schrödinger equation, we derive the wave functions and energy spectra of the system, taking into account the spin-orbit coupling effect and symmetry considerations. Numerical methods are employed to analyze the energy dispersion and spatial distribution of electronic states under varying magnetic field strengths. The results reveal the evolution of localized states, spin splitting, and magneto-dependent conductivity, offering insights into magneto-optical and transport behaviors. These findings provide a theoretical foundation for future studies on the optical properties of NLSMs in the presence of a magnetic field.

Keywords: *Landau levels, Nodal-line semimetals, Schrödinger equations.*

Cite: Huynh, V. P., & Bui, N. T. (2026). Electronic states of nodal-line semimetal under magnetic field. *Dong Thap University Journal of Science, 15*(5), 11-19. https://doi.org/10.52714/dthu.ns.2371.1829

TRẠNG THÁI ĐIỆN TỬ CỦA HỆ ĐƯỜNG NÚT BÁN KIM LOẠI TRONG TỪ TRƯỜNG

Bùi Ngọc Thu[1] và Huỳnh Vĩnh Phúc[2*]

[1]Học viên cao học, Trường Đại học Đồng Tháp, Việt Nam

[2]Khoa Sư phạm Khoa học tự nhiên, Trường Sư phạm, Trường Đại học Đồng Tháp, Việt Nam

**Tác giả liên hệ, Email: hvphuc@dthu.edu.vn*

Lịch sử bài báo

Ngày nhận: 06/5/2025; Ngày nhận chỉnh sửa: 26/6/2025; Ngày duyệt đăng: 28/6/2025

Tóm tắt

Bán kim loại đường nút (NLSM) đã thu hút được sự chú ý đáng kể do các tính chất điện tử độc đáo của chúng phát sinh từ sự xuất hiện đường nút một chiều trong không gian xung lượng. Trong nghiên cứu này, chúng tôi nghiên cứu các trạng thái điện tử của NLSM dưới ảnh hưởng của một từ trường ngoài đồng nhất. Bằng cách xây dựng và giải phương trình Schrödinger, chúng tôi suy ra các hàm sóng và phổ năng lượng của hệ, có tính đến hiệu ứng liên kết spin-quỹ đạo và tính đối xứng. Các phương pháp số được sử dụng để phân tích sự phân tán năng lượng và phân bố không gian của các trạng thái điện tử dưới các cường độ từ trường khác nhau. Kết quả cho thấy sự tiến hóa của các trạng thái cục bộ, sự phân tách spin và mật độ dòng phụ thuộc vào từ trường, cung cấp thông tin chi tiết về các hành vi quang-từ và vận chuyển. Những phát hiện này cung cấp nền tảng lý thuyết cho các nghiên cứu trong tương lai về các tính chất quang của NLSM trong từ trường.

Từ khóa: *Hệ đường nút bán kim loại, Mức Landau, Phương trình Schrödinger.*

1. Introduction

With the rapid advancement of science and technology, numerous advanced materials have been developed to replace traditional ones (Le et al., 2022; Phuc, 2023; Phuc et al., 2015). Among these, nodal-line semimetals (NLSMs) have emerged as promising candidates. NLSMs are a unique class of materials characterized by one-dimensional band crossings in their electronic structures. Unlike nodal-point semimetals, where band degeneracies occur at discrete points, NLSMs exhibit band degeneracies along continuous momentum-space lines (Yang et al., 2022). The term NLSM highlights the crucial role of these nodal lines in shaping the electronic and topological properties of the material (Buccheri et al., 2024). The band structure of NLSMs is governed by various crystal symmetries, which can enforce symmetry-protected band degeneracies. NLSMs possess distinctive electronic properties, such as non-linear electric polarization, which are absent in nodal-point semimetals (Buccheri et al., 2024). Their well-defined nodal lines result in unique features in the local density of states (LDOS), which can be explored using methods like single-particle Green's function calculations (Medeiros-Silva et al., 2025). Moreover, the electronic behavior of NLSMs can transition to that of nodal-point semimetals depending on conditions such as magnetization direction or interaction strength.

The presence of interface states further contributes to the unique electronic properties of NLSMs. These states arise at the junctions of different materials, for example, between a half-Heusler semiconductor and a semiconductor with non-localized states, where substitutional element concentrations may vary across multiple layers. Interface engineering can reveal additional states, known as dispersive drumhead states, which exist at finite energies but they are not protected by topological invariants. These states are analogous to Volkov-Pankratov states found in graphene and topological insulators, offering deeper insights into the system's electronic structure (Luo et al., 2025). When an external magnetic field is applied, the electronic states of NLSMs undergo significant modifications. The energy spectrum displays distinctive features that depend on the magnetic field strength, allowing for the classification of localized states. The coupling between the magnetic field and electron spin introduces a Zeeman term, breaking time-reversal symmetry and lifting spin degeneracy. At low temperatures, the lowest spin-polarized state dominates, while higher spin states become populated as temperature increases. The energy levels' dependence on magnetic field strength is essential for understanding electron dynamics in NLSMs. In the ground state, electrical conductivity typically increases with magnetic field strength due to the suppression of electron spin-flip scattering, which enhances overall electron mobility (Liu et al., 2019). Additionally, the presence of a fixed magnetic field, such as 14 T, modifies the magnetoresistance (MR), with temperature playing a critical role in determining the MR magnitude under different conditions (Osada et al., 2022).

In this paper, we present a detailed analysis of the electronic states of NLSMs in the presence of a uniform magnetic field, including their wave functions and energy spectra. We outline the method used to derive these states and apply numerical techniques to visualize and analyze the results. The influence of varying external magnetic fields on the wave function and energy is also explored. These findings provide a foundational basis for further investigations into other important properties of NLSMs, such as magneto-optical absorption and electronic transport behaviors.

2. Model of the system

We consider a three dimensional system of NLSM whose Hamiltonian is given as follows (Chang & Ma, 2024):

$$H = \hbar v_F k_z \sigma_x + M(k_0^2 - \vec{k}^2)\sigma_z, \quad (1)$$

where $\hbar v_F = 0.5\text{eV}\cdot\text{nm}$ is the Fermi energy, $\vec{k} = (k_x, k_y, k_z)$ is the wave vector, σ_x and σ_z are the Pauli matrices, $M = 5\ \text{eV}\cdot\text{nm}^2$ and $k_0 = 0.3\ \text{nm}^{-1}$ are the parameters of the NLSM. Physically, the parameter *M* governs the band curvature and determines the effective mass of charge carriers near the nodal line. At the same time, k_0 sets the radius of the nodal loop in momentum space in the absence of spin-orbit coupling. Both M and k_0 are material-dependent parameters that reflect the microscopic band structure of specific nodal-line semimetals. Their values can be obtained from first-principles calculations or fitting to experimental data. Incorporating a mass term Δ, primarily arising from spin-orbit coupling (SOC) (Zhang et al., 2019), into the Hamiltonian (1), we arrive at Eq. (2). It is important to note that while SOC is the dominant mechanism considered here, other symmetry-breaking perturbations-such as structural distortions or external electric fields-could also contribute to the mass term in realistic materials.

$$H = \hbar v_F k_z \sigma_x + \left[M(k_0^2 - \vec{k}^2) + \tau_z \Delta \right] \sigma_z, \quad (2)$$

where $\tau_z = \pm 1$ is the spin index. Substituting the expressions of the Pauli matrices into Eq. (2), we get

$$H = \begin{pmatrix} M(k_0^2 - \vec{k}^2) + \tau_z \Delta & \hbar v_F k_z \\ \hbar v_F k_z & -M(k_0^2 - \vec{k}^2) - \tau_z \Delta \end{pmatrix}, \quad (3)$$

The corresponding energy spectrum is the eigenvalue of the Hamiltonian operator (3), which is calculated as follows

$$E_{\pm} = \pm \sqrt{\left(\hbar v_F k_z\right)^2 + \left[M(k_0^2 - \vec{k}^2) + \tau_z \Delta \right]^2}, \quad (4)$$

where the sign $\pm$ corresponds to the conduction band and valence band of the NLSM. At the intersection of energy bands, i.e., $k_z = 0,$ the equation (4) becomes

$$E_{\pm, k_z = 0} = \pm \left| M k_0^2 + \tau_z \Delta - M\left(k_x^2 + k_y^2\right) \right|. \quad (5)$$

The results obtained in Eq. (5) show that the conduction band and the valence band touch each other at $E_+ = E_- = 0,$ when the following condition is satisfied

$$M(k_x^2 + k_y^2) = M k_0^2 + \tau_z \Delta. \quad (6)$$

This condition describes a circle in the plane (k_x, k_y) of momentum space with radius $R = \sqrt{k_0^2 + \tau_z \Delta / M}$. So the nodal line in this case is a circle. In this study, the model Hamiltonian assumes isotropic dispersion in the kx-ky plane, resulting in a circular nodal line. Consequently, the electronic properties are effectively isotropic in the absence of an external magnetic field. However, in realistic materials, the anisotropy of the band structure-arising from lower crystal symmetries-can lead to direction-dependent behaviors. Such effects are not considered in this simplified model but are of interest for future investigations.

3. Modify the electronic states of the nodal line semimetal by a magnetic field

We now turn our attention to the electronic states of the NLSM under a uniform magnetic field. Applying a magnetic field $\vec{B}=(0,0,B)$ to the *z*-direction of the NLSM. The corresponding vector potential is chosen as $\vec{A}=(0,Bx,0)$. Using the Peierls transformation, the wave vector $\vec{k}$ in Eq. (3) is replaced by

$$\vec{k}=\left(k_x,k_y+\frac{eBx}{\hbar},k_z\right)=\left(k_x,k_y+\frac{x}{\alpha_c^2},k_z\right), \tag{7}$$

where $\alpha_c=(\hbar/eB)^{1/2}$ is the magnetic length. Using the wave function (Wang et al., 2017)

$$\Psi=\left|\eta,\psi\right\rangle=\left|\chi_\eta\right\rangle\otimes\left|\psi(x)\right\rangle\otimes\left|\psi(y)\right\rangle\otimes\left|\psi(z)\right\rangle, \tag{8}$$

where $\psi(y)=e^{ik_y y}/\sqrt{L_y}$, $\eta=1,2,$ and $\chi_1=\begin{pmatrix}0\\1\end{pmatrix}$, $\chi_2=\begin{pmatrix}1\\0\end{pmatrix}$. Then the Schrödinger equation $H\Psi=E\Psi$ gives us the following equation for the *x*-direction

$$-M_{k_0}^{\tau_z}\psi(x)+M\left[-\partial_x^2+\left(k_y+\frac{x}{\alpha_c^2}\right)^2\right]\psi(x)=E_\perp\psi(x), \tag{9}$$

where we have denoted $M_{k_0}^{\tau_z}=M\cdot k_0^2+\tau_z\Delta$. The equation (9) is rewritten as follows

$$\partial_\xi^2\psi(\xi)+(\lambda-\xi^2)\psi(\xi)=0, \tag{10}$$

where $\xi=(x-x_0)/\alpha_c$, with $x_0=-\alpha_c^2k_y$, and $\lambda=(\alpha_c^2/M)(E_\perp+M_{k_0}^{\tau_z})$. The solution of the Eq. (10) is a harmonic function, that is

$$\psi_n(\xi)=N_n e^{-\xi^2/2}H_n(\xi), \tag{11}$$

where N_n is the normalization constant, $n=0,1,2,\ldots,$ is the Landau level (LL) index, and $H_n(\xi)$ is the *n*th-order Hermite polynomial. The corresponding energy is found from the condition $2n+1=\lambda,$ which leads to

$$E_\perp=\frac{2M}{\alpha_c^2}\left(n+\frac{1}{2}\right)-M_{k_0}^{\tau_z}. \tag{12}$$

Similarly, the wave function and energy in the *z*-direction are

$$\begin{aligned}&\psi_{n_z}(z)=\sqrt{\frac{2}{L_z}}\sin\left[k_z\left(z+\frac{L_z}{2}\right)\right],\ n_z=0,1,2,\ldots\\&E_z=Mk_z^2,\ k_z=\frac{n_z\pi}{L_z}.\end{aligned} \tag{13}$$

Thus, the total energy spectrum of the NLSM system is

$$E_{n,p}^{k_z,\tau_z} = p\sqrt{\left(\hbar v_F k_z\right)^2 + \left[M_{k_0}^{\tau_z} - Mk_z^2 - \frac{M}{\alpha_c^2}(2n+1)\right]^2}, \tag{14}$$

where $p = \pm 1$ is for the conduction and valence bands.

4. Numerical results and discussion

We now present our numerical results on the wave function and energy spectrum of the NLSM.

In Fig. 1, we present the LL energy spectrum described by Eq. (14) for two different values of the SOC strength with periodic boundary condition. Positive energy levels correspond to the conduction band, while negative levels correspond to the valence band. As shown in Fig. 1(a), when $\Delta = 0$, the spectra associated with $\tau_z = +1$ and $\tau_z = -1$ are identical, resulting in each LL being doubly degenerate. Furthermore, in this gapless case, the conduction and valence bands do not intersect, implying a finite bandgap in the energy spectrum.

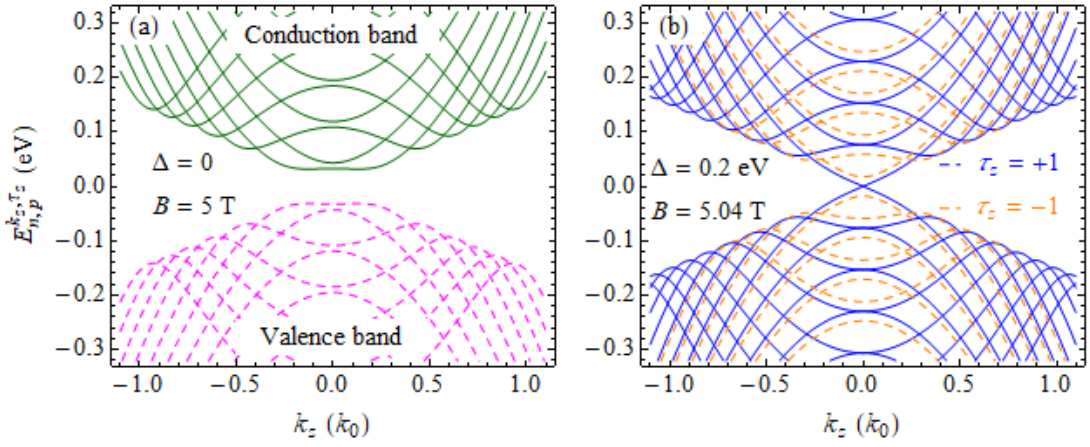

Figure 1. The dependence of the energy spectrum on the k_z for two values of SOC strength at $B = 5$ T, (a) for $\Delta = 0$, and (b) for $\Delta = 0.2$ eV.

Under Eq. (12), the conduction and valence band LLs can only touch when the energy $E_\perp = 0$, which corresponds to a specific magnetic field

$$B = B_n^{\tau_z} = \frac{\hbar(Mk_0^2 + \tau_z\Delta)}{(2n+1)eM}. \tag{15}$$

Using the model parameters of the NLSM defined below Eq. (1), we find that the magnetic field values satisfying the condition (15) are $B_5^{\pm 1} = 5.39$ T, and $B_6^{\pm 1} = 4.56$ T. Since these critical values deviate significantly from the field applied in Fig. 1(a) ($B = 5$ T), the energy gap remains open, and no LL crossing is observed in this case.

Figure 1(b) illustrates the energy spectrum for $\Delta = 0.2$ eV. In contrast to the case of $\Delta = 0$, the LLs associated with $\tau_z = \pm 1$ are now clearly split due to SOC. Notably, at $B = 5.04$ T, the condition $B = B_8^{+1}$ from Eq. (15) is satisfied, leading to a band-touching point between the conduction and valence bands. This results in the closure of the bandgap,

as clearly visible in the figure, highlighting the critical role of SOC and magnetic field in controlling the topological band structure of NLSM systems, offering potential for bandgap engineering through external tuning.

Figure 2 illustrates the dependence of the LL energy spectrum of the NLSM on the magnetic field B for two distinct values of the SOC strength Δ. The LLs are labeled in ascending order according to the LL index n. In the case of $\Delta = 0$ [Fig. 2(a)], the magnetic field values that satisfy the band-touching condition given by Eq. (15) are $B_0^{\tau_z} = 59.31$ T, $B_1^{\tau_z} = 19.77$ T, $B_2^{\tau_z} = 11.86$ T, $B_3^{\tau_z} = 8.47$ T, and so on. Notably, $B_0^{\tau_z}$ is beyond the field range considered in Fig. 1(a). These results confirm the inverse relationship between $B_n^{\tau_z}$ and the LL index n, as expressed in Eq. (15).

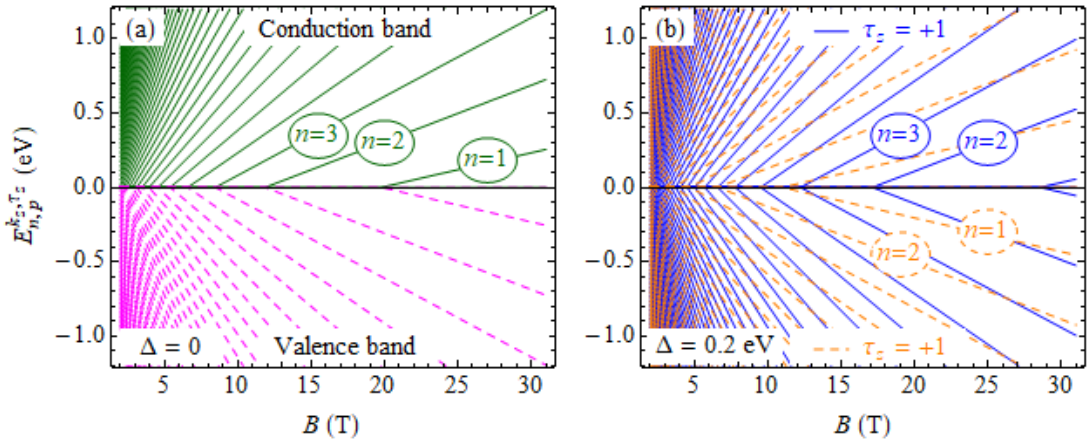

Figure 2. The dependence of the energy spectrum on the magnetic field for two values of SOC strength at $n_z = 0$, (a) for $\Delta = 0$, and (b) for $\Delta = 0.2$ eV.

For $\Delta = 0.2$ eV [Fig. 2(b)], the LLs corresponding to $\tau_z = \pm 1$ are fully split due to the SOC, as previously discussed in Fig. 1(b). The magnetic field values at which the conduction and valence bands touch, as per Eq. (15), are found to be as follows for $\tau_z = +1$: $B_0^{+1} = 85.67$ T, $B_1^{+1} = 28.56$ T, $B_2^{+1} = 17.13$ T, $B_3^{+1} = 12.24$ T,… and as follows for $\tau_z = -1$: $B_0^{-1} = 32.95$ T, $B_1^{-1} = 10.98$ T, and $B_2^{-1} = 6.59$ T,… These values again confirm the inverse scaling of $B_n^{\tau_z}$ with n, and demonstrate how the presence of SOC modifies the magnetic field dependence of LL crossings.

These observations highlight the substantial effect of SOC on the LL energy spectrum of NLSMs. As the LL structure dictates optical transitions, the SOC-induced modifications are expected to have a significant impact on the material's magneto-optical response, such as optical absorption. We will continue to study and report these results in future works.

Figure 3 presents the (a) component wavefunctions and (b) corresponding probability current densities for several of the lowest Landau levels (LLs) in the nodal-line semimetal (NLSM) system. As shown in Fig. 3(a), the spatial profiles of the wavefunctions exhibit the well-known features of quantum harmonic oscillator eigenstates, with an increasing number of nodes corresponding to higher LL indices. This structure reflects the quantization imposed by the magnetic field in the transverse direction. Correspondingly, Fig. 3(b) displays the probability current densities $J_n(\xi)$, which also follow patterns characteristic of harmonic

oscillator modes. These currents demonstrate oscillatory behavior and are localized in real space, consistent with the magnetic confinement of charge carriers. The profiles of both the wavefunctions and current densities confirm the harmonic oscillator nature of the LL quantization in this system and provide insight into the spatial dynamics that underlie the optical transition matrix elements discussed in future works.

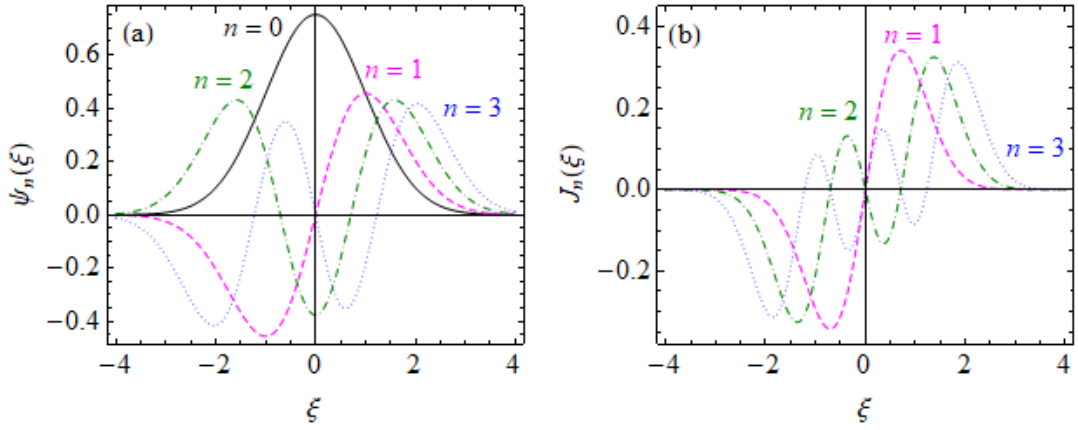

Figure 3. (a) The component wave function $\psi_n(\xi)$ and (b) the corresponding probability current density $J_n(\xi)$ for some first LLs.

5. Conclusion

In this study, we have presented a comprehensive analysis of the electronic states in NLSM subjected to a uniform magnetic field. By deriving the wave function and energy spectrum through analytical and numerical methods, we identified key features such as spin degeneracy lifting, SOC-induced spectral shifts. The study also highlights the emergence of interface-induced states and their behavior under external field modulation. Our results not only deepen the understanding of the magnetic response in NLSMs but also lay the groundwork for further exploration of their magneto-optical and transport properties.

Acknowledgements: This research is supported by the project B2025-SPD-07.

References

Buccheri, F., Egger, R., & De Martino, A. (2024). Dispersive drumhead states in nodal-line semimetal junctions. *Physical Review Research*, *6*, 013193. https://doi.org/10.1103/PhysRevResearch.6.013193

Chang, M., & Ma, R. (2024). Anisotropic three-dimensional quantum Hall effect in topological nodal-line semimetals. *Physical Review B*, *110*(4), 045413. https://doi.org/10.1103/PhysRevB.110.045413

Le, T. H., Tran, N. B., Nguyen, N. H., Le, T. N. T., & Huynh, V. P. (2022). Dirac electron in gapped graphene under exponentially decaying magnetic field. *Tạp chí Khoa học Đại học Đồng Tháp*, *11*(5), 35-40. https://doi.org/10.52714/dthu.11.5.2022.978

Liu, J., Liu, P., Gordon, K., Emmanouilidou, E., Xing, J., Graf, D., Chakoumakos, B. C., Wu, Y., Cao, H., Dessau, D., Liu, Q., & Ni, N. (2019). Nontrivial topology in the layered Dirac nodal-line semimetal candidate $SrZnSb_2$ with distorted Sb square nets. *Physical Review B*, *100*(19), 195123. https://doi.org/10.1103/PhysRevB.100.195123

Luo, B.-B., Gao, M.-J., & An, J.-H. (2025). Topological semimetal with coexisting nodal points and nodal lines. *arXiv preprint arXiv:2501.13636*.

Medeiros-Silva, A. R., Malard, M., Pereira, R. G., & Paiva, T. (2025). Magnetism in symmetry-enforced nodal-line semimetals. *arXiv preprint arXiv:2501.12187*.

Osada, T., Ochi, T., & Taen, T. (2022). Thermoelectric Hall effect at high-magnetic-field quantum limit in graphite as a nodal-line semimetal. *Journal of the Physical Society of Japan*, *91*(6), 063701. https://doi.org/10.7566/JPSJ.91.063701

Phuc, H. V. (2023). Two-photon magneto-optical transitions in quantum rings. *Journal of Applied Physics*, *133*(7). https://doi.org/10.1063/5.0138500

Phuc, H. V., Hieu, N. N., Dinh, L., & Phong, T. C. (2015). Nonlinear optical absorption in parabolic quantum well via two-photon absorption process. *Optics Communications*, *335*, 37-41. https://doi.org/https://doi.org/10.1016/j.optcom.2014.09.004

Wang, C. M., Sun, H.-P., Lu, H.-Z., & Xie, X. C. (2017). 3D quantum hall effect of Fermi arcs in topological semimetals. *Physical Review Letters*, *119*(13), 136806. https://doi.org/10.1103/PhysRevLett.119.136806

Yang, M.-X., Wei, L., & and Chen, W. (2022). Quantum transport in topological nodal-line semimetals. *Advances in Physics: X*, *7*, 2065216. https://doi.org/10.1080/23746149.2022.2065216

Zhang, X., Fu, B., Jin, L., Dai, X., Liu, G., & Yao, Y. (2019). Topological nodal line electrides: Realization of an ideal nodal line state nearly immune from spin–orbit coupling. *The Journal of Physical Chemistry C*, *123*(42), 25871-25876. https://doi.org/10.1021/acs.jpcc.9b08446